Journal of Inflammation Research

Dovepress
Taylor & Francis Group

Open Access Full Text Article

RESEARCH LETTER

# Evaluation of NETosis Inhibitors in a Laboratory-Developed ex-vivo Human Neutrophil Model

Constant Gillot[1], Pauline Michaux[1], Jonathan Decarpentrie[1], Romane Vandamme[1], Jean-Michel Dogné[1], Julien Favresse[1,2], Jonathan Douxfils[1,3]

[1]Clinical Pharmacology and Toxicology Research Unit, Namur Research Institute for Life Sciences, University of Namur, Namur, 5000, Belgium; [2]Department of Laboratory Medicine, Clinique St-Luc Bouge, Namur, 5000, Belgium; [3]Qualiblood s.a., Research and Development Department, Liège, 4000, Belgium

Correspondence: Constant Gillot, Email constant.gillot@unamur.be



## Introduction

Neutrophils are central players in the innate immune system, primarily defending the host through phagocytosis, degranulation, and the release of inflammatory mediators. In 2004, a fourth mechanism was identified: the formation of neutrophil extracellular traps (NETs).[1] These extracellular web-like structures are composed of decondensed chromatin fibers (cell free DNA (cfDNA)) decorated with histones and granular enzymes such as neutrophil elastase (NE), myeloperoxidase (MPO), and cathepsin G.[1] The release process, termed NETosis, involves reactive oxygen species (ROS) generation, chromatin decondensation facilitated by peptidyl-arginine deiminase 4 (PAD4), and the rupture of nuclear and plasma membranes, allowing the extrusion of NETs into the extracellular space.[2] Although initially described as a defense mechanism against pathogens, NETosis is now recognized as a double-edged sword. Excessive or dysregulated NET formation contributes to sterile inflammation, promotes thrombosis, and may lead to tissue damage in various pathologies, including acute respiratory distress syndrome (ARDS) and autoimmune diseases.[3] These detrimental effects have sparked growing interest in pharmacological inhibition of NETosis as a therapeutic strategy. Among the agents under investigation, Cl-amidine, an irreversible PAD4 inhibitor, and sivelestat, a selective NE inhibitor, have shown potential in limiting NET formation in preclinical studies.[4] In this work, we aim to evaluate the inhibitory effects of Cl-amidine and sivelestat on NETosis using an ex vivo laboratory-developed model, offering insight into their potential therapeutic utility.

## Materials and Methods

### Blood Collection

Peripheral blood was collected in EDTA-coated tubes (BD Vacutainer $K_2$EDTA, Becton Dickinson, New Jersey, USA) from 3 healthy donors. A written consent was obtained from volunteers and blood collection was carried out in accordance with the ethical agreement of the institution (CHU UCL NAMUR, ethical approval number B03920096633). Blood samples were registered in a notified biobank (NAB-X, notified at the Federal Agency for Medicines and Health Products (FAMHP) under the registration number BB190116). This study is in accordance with the declaration of Helsinki.

### Neutrophil Extraction

Human neutrophils were isolated from peripheral blood using the MACSx-press® kit (Miltenyi Biotec, cat. no.: 130–104-434). After washing, cells were resuspended in 25 mL of 10× diluted red blood cell lysis buffer (Miltenyi Biotec, cat. no.: 130–094-183) and centrifuged at 160 × g for 5 minutes. The pellet was then resuspended in 20 mL of RPMI with L-glutamine (Westburg, cat. no.: CA RPMI-A). Neutrophils were counted via trypan blue exclusion using a Neubauer

https://doi.org/10.2147/JIR.S571649
Received: 2 October 2025
Accepted: 16 December 2025
Published: 30 January 2026

chamber (Leica) and adjusted to $2 \times 10^6$ cells/mL. Neutrophil viability and purity were assessed by flow cytometry to ensure that no necrosis or apoptosis occurred during the extraction procedure. Cell viability was evaluated by propidium iodide (PI) exclusion, distinguishing viable cells with low PI signal from dead cells with high fluorescence, which were excluded from the analysis. Leukocytes were identified using CD45 staining, and neutrophils were subsequently gated based on CD15 expression. Neutrophil activation was assessed using CD66b (a well-established activation marker rapidly upregulated on neutrophil upon activation), and the mean fluorescence intensity (MFI) was calculated within the gated neutrophil population.

## NETs Analysis

The neutrophil extract solution was treated with DNase to prevent interference with Sytox Green reading. NETosis was induced in 96-well black tissue culture plates by combining 112.5 µL of neutrophil suspension with 112.5 µL of TNF-α (20 µM; ThermoFisher Scientific, cat. no.: A42552) per well. For inhibition assays, 25 µL of either sivelestat (Sigma-Aldrich, cat. no.: S7198-5MG) or Cl-Amidine (Sigma-Aldrich, cat. no.: 506282–10MG) was added at final concentrations of 10, 100, or 1000 nM or 35, 350 or 3500 nM, respectively through dilutions in RPMI. Positive controls contained 112.5 µL of neutrophils suspension and 112.5 µL TNF-α solution with 25 µL of RPMI, while negative controls received 137 µL of RPMI without inducer or inhibitor. Each condition was tested in three independent experiments using neutrophils isolated from three different healthy donors, with each condition performed in triplicate wells per experiment. NET formation was quantified using two fluorescent markers: Sytox Green (ThermoFisher, cat. no.: R37168), specific for cell-free DNA, and the NE-specific peptide Me-OSuc-Ala-Ala-Pro-Val-AFC (Anaspec, cat. no.: AS-24141) at a final concentration of 1.6 µM. To avoid signal interference, each well received only one marker. Calibration curves were established for cfDNA fluorescence to allow quantitative analysis of NETosis. Fluorescence was recorded every 2 minutes for 8 hours using a SpectraMax iD3 microplate reader (Molecular Devices), with excitation/emission settings of 504/523 nm for Sytox Green and 380/500 nm for NE activity.

## Statistical Analysis

Mean and the 95% confidence interval (CI) were used to present the data. The time required to reach 50% DNA release/NE activity ($T_{50}$) was computed, and the area under the curve (AUC) was also calculated. Km and Vmax were determined for the evaluation of NE activity. NE activity data were normalized to the condition exhibiting the highest RFU value, which in this case corresponded to the positive control, and expressed as a percentage. Normality of the results was assessed using the Kolmogorov–Smirnov test. To evaluate the presence of significant differences between the different molecules tested and the positive control condition, a one-way ANOVA was performed followed by Dunnett's post-hoc test. A p-value $< 0.05$ was considered statistically significant. Analyses were conducted using GraphPad Prism version 10.0.3.

# Results

cfDNA release, measured by Sytox Green, followed a sigmoidal kinetic profile, whereas NE activity, assessed with Me-OSuc-Ala-Ala-Pro-Val-AFC, exhibited Michaelis–Menten kinetics (Figure 1). In positive control conditions, cfDNA release reached $T_{50}$ at 186.9 min (95% CI: 181.5–192.7 min). In the presence of sivelestat, $T_{50}$ increased in a dose-dependent manner, from 203.7 min (95% CI: 201.1–206.3 min) at 10 nM to 254.0 min (95% CI: 252.2–255.9 min) at 1000 nM. (Figure 1A and Table 1) Maximal cfDNA release ranged from 2.81 µg/mL (95% CI: 2.78–2.85) at 100 nM to 2.67 µg/mL (95% CI: 2.65–2.69) at 1000 nM. (Table 1) NE activity was more strongly affected: the 10 nM condition was the only one to reach the 50% activity threshold ($T_{50}$ = 427.0 min, 95% CI: 405.8–448.2), whereas higher concentrations resulted in a stronger inhibition of NE activity, reflected by a progressive decrease in Vmax from 80.4%/min (95% CI: 67.7–106.0) at 10 nM to 15.7%/min (95% CI: 15.2–16.2) at 1000 nM, compared to 104.5%/min (95% CI: 102.4–106.8) in the positive control. (Figure 1B and Table 1) Regarding the total amount of DNA release or NE activity, all tested concentration of sivelestat demonstrated a significant reduction ($p < 0.001$). With Cl-amidine, $T_{50}$ for cfDNA release also increased, from 244.5 min (95% CI: 239.5–249.7) at 35 nM to 265.8 min (95% CI: 263.8–267.9) at 3500 nM, with maximal release between 3.15 µg/mL (95% CI: 3.08–3.22) and 3.00 µg/mL (95% CI: 2.97–3.03). (Figure 1C and Table 1) NE activity was only

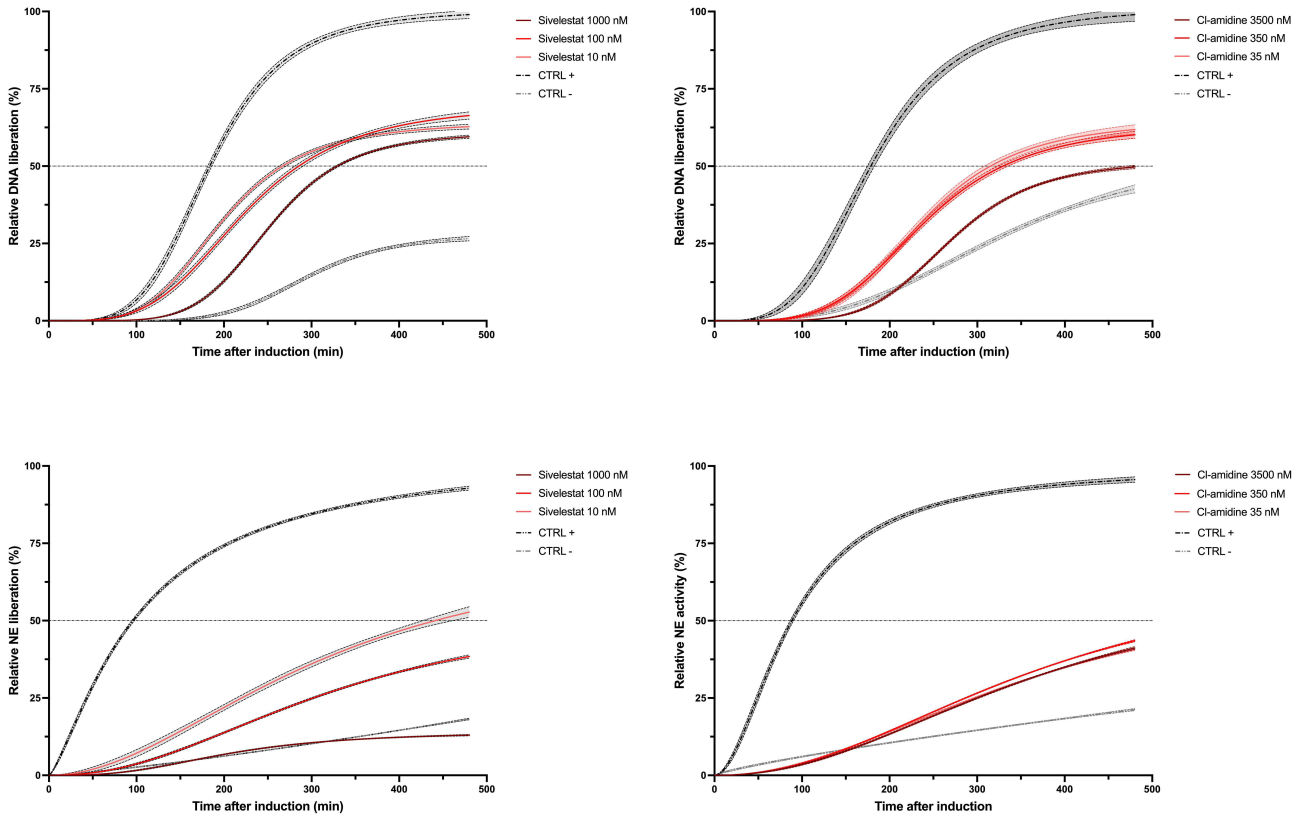


**Figure 1** (Upper left) Concentration of cdDNA as function of time after NETosis induction with Sivelestat as potential inhibitor. (Bottom left) Evolution of the NE activity as function of time after NETosis with Sivelestat as potential inhibitor. (Upper right) Concentration of cdDNA as function of time after NETosis induction with Cl-amidine as potential inhibitor. (Bottom right) Evolution of the NE activity as function of time after NETosis with Cl-amidine as potential inhibitor.

mildly reduced, with Vmax ranging from 73.6%/min (95% CI: 69.9–78.0) to 69.1%/min (95% CI: 64.2–75.3). (Figure 1D and Table 1) Regarding the total amount of DNA release or NE activity, all tested concentration of Cl-amidine demonstrated a significant reduction ($p < 0.001$). None of the tested concentrations for Cl-Amidine cross the 50% activity threshold compared to the positive control. These results support distinct mechanisms: sivelestat directly inhibits NE, whereas Cl-amidine acts upstream in the NETosis cascade.

## Discussion

This study reinforces the importance of multiparametric analyses in NETosis research, revealing distinct yet complementary profiles for DNA release and NE activity. The sigmoidal kinetic pattern observed for DNA release reflects the sequential nature of chromatin decondensation and extrusion, while NE activity followed classical Michaelis-Menten kinetics, consistent with its catalytic function during granule exocytosis. These divergent profiles support the need to monitor multiple NETosis biomarkers to capture the full dynamics of the process. Sivelestat exhibited a robust inhibitory effect on NE activity, while cfDNA $T_{50}$ values showed only a modest shift, indicating a limited impact on NET formation kinetics. These findings are consistent with prior studies highlighting NE's central role in promoting inflammatory injury in acute respiratory distress syndrome and COVID-19.[5,6] Notably, the dose-dependent inhibition observed in our model strengthens the case for NE inhibition as a pharmacologically tractable strategy to mitigate NET-associated tissue damage. However, our results also show that sivelestat's impact on chromatin structure was more limited, indicating that enzymatic inhibition alone may not fully disrupt NET architecture. These differences arise from the distinct mechanisms of action of the two inhibitors: sivelestat targets NE activity at a downstream stage of NETosis, whereas Cl-amidine acts upstream by blocking PAD4-dependent chromatin decondensation. Consequently, each compound affects different steps of NET formation, explaining the divergent kinetic profiles observed. In contrast, Cl-amidine selectively reduced DNA release, consistent with its action on PAD4, a key upstream mediator of histone citrullination and


https://doi.org/10.2147/JIR.S571649

**Table 1** Comparison of the $T_{50}$, Total cfDNA Release and Vmax to Positive Control Between the Two Potential Inhibitors Investigate

| | **DNA Release** | | | | | | | | | |
|---|---|---|---|---|---|---|---|---|---|---|
| | **Sivelestat** | | | | | **Cl-Amidine** | | | | |
| | **1000 nM** | **100 nM** | **10 nM** | **Positive Control** | **Negative Control** | **3500 nM** | **350 nM** | **35 nM** | **Positive Control** | **Negative Control** |
| **$T_{50}$ (min) *(95% CI)*** | 254.0 *(252.2–255.9)* | 282.3 *(262.4–302.1)* | 203.7 *(201.1–206.3)* | 186.9 *(181.5–192.7)* | NA | 472.5 *(454.2–490.8)* | 335.3 *(262.4–420.6)* | 325.8 *(261.1–390.4)* | 186.9 *(181.5–192.7)* | NA |
| **Total cfDNA release (µg/mL) *(95% CI)*** | 2.67 *(2.65–2.69)* | 2.81 *(2.78–2.84)* | 2.73 *(2.70–2.76)* | 5.02 *(4.90–5.17)* | 2.51 *(2.35–2.74)* | 3.00 *(2.97–3.03)* | 3.06 *(2.96–3.18)* | 3.15 *(3.08–3.22)* | 5.02 *(4.90–5.17)* | 2.51 *(2.35–2.74)* |
| | **NE Activity** | | | | | | | | | |
| | **Sivelestat** | | | | | **Cl-Amidine** | | | | |
| | **1000 nM** | **100 nM** | **10 nM** | **Positive Control** | **Negative Control** | **3500 nM** | **350 nM** | **35 nM** | **Positive Control** | **Negative Control** |
| **$T_{50}$ (min) *(95% CI)*** | NA | NA | 427.0 *(405.8–448.2)* | 95.3 *(53.1–137.6)* | NA | NA | NA | NA | 84.5 *(69.7–99.3)* | NA |
| **Vmax (%/min) *(95% CI)*** | 15.7 *(15.2–16.2)* | 64.9 *(60.0–71.3)* | 80.4 *(20.3–56.2)* | 104.5 *(102.4–106.8)* | 12.0 *(10.7–13.2)* | 69.1 *(64.2–75.3)* | 73.7 *(69.9–78.0)* | 72.8 *(68.0–78.7)* | 99.7 *(98.0–101.5)* | 16.4 *(10.7–22.0)* |


https://doi.org/10.2147/JIR.S571649

chromatin decondensation.[7] Its minimal effect on NE activity highlights the distinct and non-redundant roles of these two enzymes in the NETosis cascade. This mechanistic specificity supports a tailored therapeutic approach, where inhibitors like Cl-amidine could be prioritized in pathologies where chromatin remodeling is predominant, such as autoimmune diseases or thrombo-inflammatory syndromes.[6] Although both Cl-amidine and sivelestat have been shown to reduce NET formation, some studies report variable efficacy depending on the experimental model, the type of inducer, and the readouts used. These discrepancies likely reflect differences in study design and highlight the importance of standardized approaches to accurately assess their inhibitory potential. Potential confounders such as cytotoxicity, reduced viability, or fluorescence interference were ruled out. PI-based flow cytometry confirmed cell viability, vehicle controls excluded solvent effects, and no interference with the DNA dye was detected, supporting genuine NETosis inhibition. Immunofluorescence imaging confirmed the biochemical findings, with both inhibitors significantly reducing chromatin filament length a hallmark of impaired NETosis. The use of a controlled ex vivo model proved particularly advantageous for dissecting these drug effects, as it allowed precise pharmacodynamic assessment, free from the systemic confounders present in in vivo models. This platform thus offers valuable translational potential for early-stage drug evaluation. Looking ahead, the development of combinatory strategies targeting both NE and PAD4 may yield synergistic benefits by blocking multiple stages of NET formation. Furthermore, integrating components such as platelets and coagulation factors into the ex vivo model would better simulate the thrombo-inflammatory context where NETs contribute to pathogenesis, including in diseases like venous thromboembolism and atherosclerosis.[6]

## Disclosure

Mr Jonathan Decarpentrie reports grants from BioWin - Waloon Region, outside the submitted work. The authors report no other conflicts of interest in this work. The abstract of this paper was presented at the BSTH2023 as a conference talk with interim findings.

(https://researchportal.unamur.be/en/publications/evaluation-of-sivelestat-as-a-netosis-inhibitor-using-an-in-house/)

## References


1. Brinkmann V, Reichard U, Goosmann C, et al. Neutrophil extracellular traps kill bacteria. *Science*. 2004;303(5663):1532–1535. doi:10.1126/science.1092385
2. Thiam HR, Wong SL, Qiu R, et al. NETosis proceeds by cytoskeleton and endomembrane disassembly and PAD4-mediated chromatin decondensation and nuclear envelope rupture. *Proc Natl Acad Sci U S A*. 2020;117(13):7326–7337. doi:10.1073/pnas.1909546117
3. Granger V, de Chaisemartin L, Chollet-Martin S. Miraculous catch by neutrophils NETs. *Med Sci*. 2014;30(5):544–549. doi:10.1051/medsci/20143005018
4. Huang J, Hong W, Wan M, Zheng L. Molecular mechanisms and therapeutic target of NETosis in diseases. *MedComm*. 2022;3(3):e162. doi:10.1002/mco2.162
5. Li Y, Zhao J, Wei J, et al. Neutrophil elastase inhibitor (Sivelestat) in the treatment of acute respiratory distress syndrome induced by COVID-19: a multicenter retrospective cohort study. *Respir Res*. 2025;26(1):28. doi:10.1186/s12931-025-03100-4
6. Zhou Y, Xu Z, Liu Z. Impact of neutrophil extracellular traps on thrombosis formation: new findings and future perspective. *Front Cell Infect Microbiol*. 2022;12:910908. doi:10.3389/fcimb.2022
7. Leshner M, Wang S, Lewis C, et al. PAD4 mediated histone hypercitrullination induces heterochromatin decondensation and chromatin unfolding to form neutrophil extracellular trap-like structures. *Front Immunol*. 2012;3:307. doi:10.3389/fimmu.2012.00307